Ranta, Mikaela; Hinkkanen, Marko; Belahcen, Anouar; Luomi, Jorma

Inclusion of hysteresis and eddy current losses in nonlinear time-domain inductance models

Published in:
37th Annual Conference of the IEEE Industrial Electronics Society (IECON)

DOI:
10.1109/IECON.2011.6119596

Published: 07/11/2011

Document Version
Peer-reviewed accepted author manuscript, also known as Final accepted manuscript or Post-print

Inclusion of Hysteresis and Eddy Current Losses in Nonlinear Time-Domain Inductance Models

Mikaela Ranta, Marko Hinkkanen, Anouar Belahcen, and Jorma Luomi
Aalto University School of Electrical Engineering
P.O. Box 13000, FI-00076 Aalto, Finland

***Abstract*—A time-domain model including the core losses of a nonlinear inductor is proposed. The model can be seen as a parallel combination of a nonlinear inductance modelling the saturation and a nonlinear resistance modelling the core losses. The desired steady-state core-loss profile is used to determine the resistance function. The model is easy to implement and can be used in many different applications. The hysteresis loop of an electrical steel sample is measured at several frequencies in order to experimentally verify the model. It is shown that the model is able to predict both major and minor hysteresis loops very well.**

I. Introduction

Modelling of nonlinear hysteretic inductances has challenged researchers for many years. A good accuracy can indeed be achieved by a physical in-depth analysis, but the resulting differential equations are very complicated. In, for instance, design and real-time control of electric drives and power electronic devices, dynamic time-domain models that are easy to implement and tune are desirable. The increasing demand for energy efficiency makes the need for accurate models of losses even larger in the future.

The core losses can be divided into three parts: hysteresis losses, classical eddy current losses and excess losses. The hysteresis losses are proportional to the frequency, while the classical eddy current losses and the excess losses are proportional to the frequency raised to the second and 1.5th power, respectively.

A generally used and very simple model of the core losses of an inductance is a constant resistance in parallel to the inductance. In the case of a sinusoidal waveform, the power dissipated in a constant resistor is proportional to the square of the frequency. This frequency dependency corresponds to the classical eddy current losses. Particularly at lower frequencies, the hysteresis losses constitute a significant part of the total core losses, and the losses predicted by a constant resistance deviate remarkably from the actual losses.

Several methods have been developed to achieve more accurate models. A general framework for modelling of hysteresis utilizing a dissipating function and a restoring function was presented in [1], [2], but no explicit function was given. In [3] a polynomial function was used to model the hysteresis loop assuming sinusoidal voltage excitation. A polynomial model for the B-H relation using the concept of a hysteresis related field intensity was proposed in [4]. In [5], a system of differential equations was developed based on the idea of separating the magnetic field into two parts, where one part represents the magnetization and the other part the hysteresis losses. In [6], the major hysteresis loop is produced by displacing the magnetizing curve while minor hysteresis loops are produced by adding reduction factors to the magnetizing curve function.

In this paper, the core losses are modelled according to the principles in [1], [2]. The dissipating function is derived based on the desired steady-state core-loss profile. The hysteresis losses and the eddy-current losses are included in the model, but, in principle, any kind of core-loss profile could be applied. A similar approach is used in [7] for the case of stator core loss modelling in induction machines. The model can easily be tuned and implemented in different applications. The hysteresis loop of an electrical steel sample is measured using an Epstein frame in order to experimentally verify the proposed model. It is shown that the model can produce major as well as minor hysteresis loops, and the predicted loops show very good agreement with the measured ones.

II. Steady-State Model

At sufficiently low freqencies, the core losses can be modelled as

$$P_{\mathrm{Fe}} = P_{\mathrm{Ft}} + P_{\mathrm{Hy}} = \frac{\omega^2 \Psi^2}{R_{\mathrm{Ft}}} + \alpha \frac{\omega \Psi^2}{R_{\mathrm{Ft}}} \tag{1}$$

where P_{Ft} denotes the eddy current losses and P_{Hy} the hysteresis losses. The parameter α determines the ratio between the two loss components: at the angular frequency $\omega = \alpha$, the eddy-current losses equal the hysteresis losses. The excess losses are here omitted for simplicity. The model can only be used in steady state, as the angular frequency ω is irrelevant in transient and in case of a non-sinusoidal flux linkage.

III. Dynamic Models

A. Lossless Nonlinear Inductance

In the dynamic model of an inductor, two main phenomena need to be included: magnetic saturation and core losses. Conventionally, the core losses are modeled using a resistor in parallel to the inductor as depicted in Fig. 1(a). Hence, the magnetic saturation can be modelled separately from the core losses.

In time-domain models, the magnetization curve can be represented as a look-up table or an explicit function can be

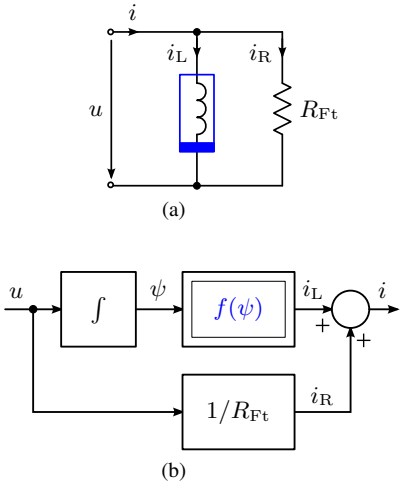

Fig. 1. Nonlinear inductor with a constant core-loss resistor: (a) circuit model; (b) and block diagram.

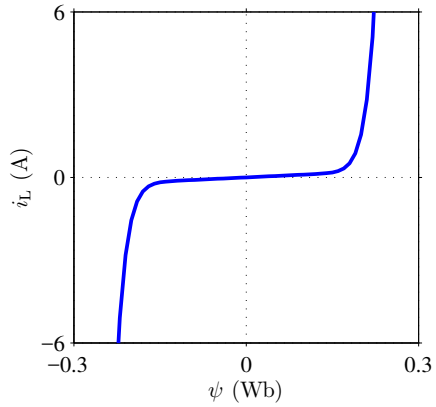

Fig. 2. Magnetization curve $i_L = f(\psi)$. Parameters values are $L_u = 0.99$ H, $\beta = 0.17$ Wb, and $S = 12.4$.

used. In this paper, the magnetizing curve is modeled using a power function [8]

$$\begin{aligned} i_L &= f(\psi) \\ &= \frac{1 + |\psi/\beta|^S}{L_u}\psi \end{aligned} \tag{2}$$

where L_u is the unsaturated inductance, and S and β are nonnegative constants. The parameter S determines the shape of the curve. At $\psi = \beta$, the inductance is half of the unsaturated value L_u. In Fig. 2, an example of the saturation curve is shown.

B. Constant Core-Loss Resistor

In the case of a constant resistor in parallel to the inductor, the instantaneous terminal current is given as

$$i = i_L + i_R = f(\psi) + \frac{u}{R_{Ft}}$$

The corresponding block diagram is shown in Fig. 1(b). The instantaneous losses can be obtained from

$$p_{Fe} = u i_R = \frac{u^2}{R_{Ft}} \tag{3}$$

Assuming sinusoidally varying flux linkage, the average losses in steady state can be expressed as

$$P_{Fe} = \frac{\omega^2 \Psi^2}{R_{Ft}} \tag{4}$$

It can be seen that the dependency of these losses on the frequency and the flux linkage corresponds to the eddy-current losses according to (1).

C. Inclusion of Hysteresis Losses Using A Nonlinear Resistance

In order to include the hysteresis losses, a nonlinear resistor is used instead of the constant resistor as depicted in Fig. 3(a) [1], [2]. The function defining the nonlinear resistor is developed based on the steady-state losses given in (1). The corresponding instantaneous losses can be written as

$$p_{Fe} = u \underbrace{\left(\frac{u}{R_{Ft}} + \frac{\alpha |\psi| \mathrm{sgn}(u)}{R_{Ft}} \right)}_{i_R = g(u,\psi)} \tag{5}$$

The dissipation function $g(u, \psi)$ can be classified as a first-order voltage-controlled nonlinear conductance [9] or a memristive system [10]. The instantaneous terminal current is given as

$$i = i_L + i_R = f(\psi) + g(u, \psi) \tag{6}$$

where the core-loss current is

$$i_R = g(u, \psi) = \frac{u}{R_{Ft}} + \frac{\alpha |\psi| \mathrm{sgn}(u)}{R_{Ft}} \tag{7}$$

Only one additional parameter, α, is needed to include the hysteresis losses as compared to the model with a constant resistor. The nonlinear resistance corresponding to (7) can be interpreted as a parallel connection of two resistances: the constant resistance R_{Ft} related to the eddy-current losses and the voltage- and flux-dependent nonlinear resistance

$$R_{Hy}(u, \psi) = \frac{R_{Ft}}{\alpha} \left| \frac{u}{\psi} \right| \tag{8}$$

related to the hysteresis losses. An example of the current as a function of the voltage is shown in Fig. 4 at two different flux levels. If the losses would be modelled using only a constant resistor, a straight line would be obtained. Due to the hysteresis losses, the current is increased proportionally to the flux.

Assuming sinusoidally varying flux linkage, the average losses in steady state can be expressed as

$$P_{Fe} = \frac{\omega^2 \Psi^2 + \alpha \omega \Psi^2}{R_{Ft}} \tag{9}$$

i.e. they correspond to (1).

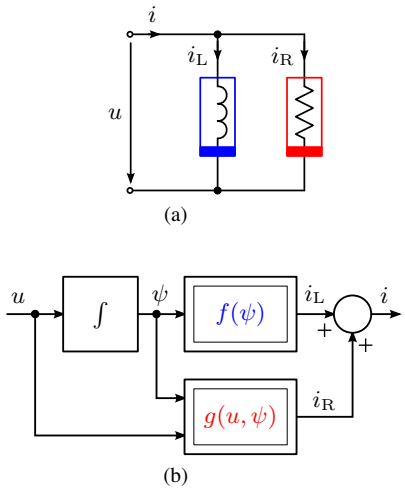

Fig. 3. Nonlinear inductor with a nonlinear core-loss resistor: (a) circuit model; (b) and block diagram.

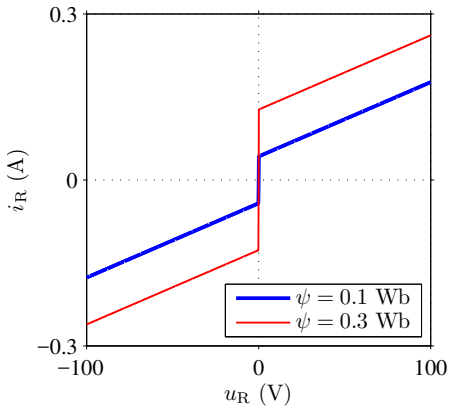

Fig. 4. Characteristics $i_R = g(u_R, \psi)$ of the nonlinear core-loss resistor. Parameters values are $R_{Ft} = 744.6\ \Omega$ and $\alpha = 315.2$ rad/s.

D. Augmented Model

The model can be easily augmented with, for example, series resistance R' and inductance L' as shown in Fig. 5(a). The corresponding state-space representation is

$$L'\frac{\mathrm{d}i}{\mathrm{d}t} = u - R'i - h(i_R, \psi) \tag{10}$$

$$\frac{\mathrm{d}\psi}{\mathrm{d}t} = h(i_R, \psi) \tag{11}$$

where $i_R = i - f(\psi)$. The voltage over the nonlinear current-controlled resistance is obtained from

$$u_R = h(i_R, \psi) = \begin{cases} 0, & \text{if } |i_R| \le \dfrac{\alpha|\psi|}{R_{Ft}} \\ R_{Ft}\left[i_R - \dfrac{\alpha|\psi|\mathrm{sgn}(i_R)}{R_{Ft}}\right], & \text{otherwise} \end{cases} \tag{12}$$

This dissipation function is reciprocal of the voltage-controlled conductance $i_R = g(u_R, \psi)$ in (7). The block diagram of the augmented model is shown in Fig. 5(b).

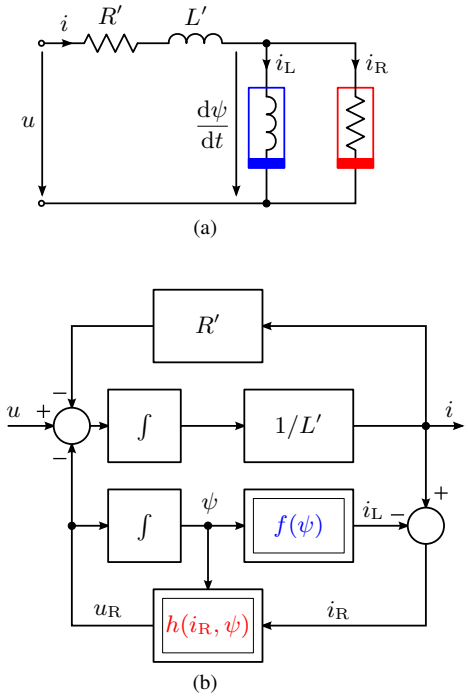

Fig. 5. Augmented inductor model: (a) circuit model; (b) and block diagram.

IV. Results

A. Experimental Setup

The measurement setup consisted of a standard 28 cm Epstein frame fed from a PC-controlled power-amplifier and a shunt for current measurement. Non oriented electrical steel designated as M400-50A was used in the experiments. A simplified diagram of the Epstein frame is shown in Fig. 6.

The control and data acquisition procedure on the PC was implemented in LabView programming environment in two parts. The first part consisted of a Virtual Instrument, which was running on a separate real-time 16-bits data-acquisition card from National Instruments. The second part, which consisted of a host program running on the PC and communicating with the card through the PCI-bus, was used to set the control parameters and save the data to the computer.

The procedure allowed the generation of signals with two separately controlled frequency components with different voltage levels and phase angles. The acquired data consisted of the instantaneous current in the primary coil of the Epstein frame and the instantaneous voltage of its secondary coil. The measurements were carried out with signals having different frequency components at different voltage levels and phase angles. Some of the measurement results are presented altogether with the simulation results for comparison purposes.

B. Parameter Identification

The hysteresis loop of an electrical steel sample was measured at several frequencies. Data recorded at the frequency 100 Hz was used to identify the saturation model and the core-loss model using data fitting. Data recorded at other frequencies was used for validation.

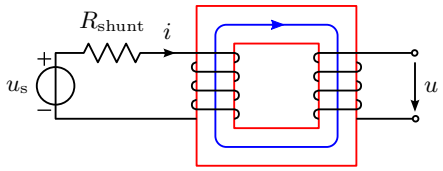

Fig. 6. Principle of the Epstein frame used in the experiments. The excitation voltage is u_{s}. The current i in the primary coil and the voltage u of the secondary coil are measured. For simplicity, the compensation of the leakage flux is not included in the figure.

In the proposed model, the terminal current consists of two components: i_{L} is related to the saturation characteristics and i_{R} corresponds to the core losses. It is assumed, that the hysteresis loop is symmetric and the magnetizing curve is situated in the middle of the hysteresis loop. Therefore, the saturation parameters can be identified irrespective of the core-loss parameters based on the total current $i = i_{\mathrm{L}} + i_{\mathrm{R}}$.

The parameters of the saturation function (2) were obtained by minimizing

$$J_L(L_{\mathrm{u}}, \beta, S) = \sum_{n=1}^{N} \left[i_n - \frac{1 + |\psi_n/\beta|^S}{L_{\mathrm{u}}} \psi_n \right]^2 \qquad (13)$$

The number of samples N was 2116 corresponding to one period. The resulting parameter values were $L_{\mathrm{u}} = 0.99$ H, $\beta = 0.17$ Wb and $S = 12.4$.

The core-loss parameters are identified in two steps. At zero flux, the current i_{L} is zero and the current i_{R} corresponds to u/R_{Ft}, where u is the voltage over the inductor. The core loss resistance can, thus, be obtained from

$$R_{\mathrm{Ft}} = \frac{u}{i}\Big|_{\psi=0} \qquad (14)$$

A moving-average filter was applied to remove the ripple in the current prior to the resistance calculation. During one period, the flux equals zero at two time instants. The resistance was calculated as the mean value of the resistance values obtained from (14) at these moments. The resulting value of R_{Ft} was 744.6 Ω.

As the resistance R_{Ft} is known, the only unknown parameter is α. This parameter is obtained by minimizing

$$J(\alpha) = \sum_{n=1}^{N} \left[p_n - u_n \left(i_{\mathrm{L},n} + \frac{u_n}{R_{\mathrm{Ft}}} + \frac{\alpha |\psi_n| \mathrm{sgn}(u_n)}{R_{\mathrm{Ft}}} \right) \right]^2 \qquad (15)$$

where the instantaneous power $p = ui$ and the current i_{L} is obtained from (2) using the parameter values obtained above. The result was $\alpha = 315.2$ rad/s.

The resistance R_{Ft} could be obtained simultaneously as the parameter α. The left-hand side of (15) would then be $J(R_{\mathrm{Ft}}, \alpha)$ while the right-hand side would be left unchanged. This, however, would lead to a higher value of R_{Ft} and the estimated hysteresis loop would have an unrealistic shape in the vicinity of zero flux as a result. A good curve shape can be ensured in a two-step identification process.

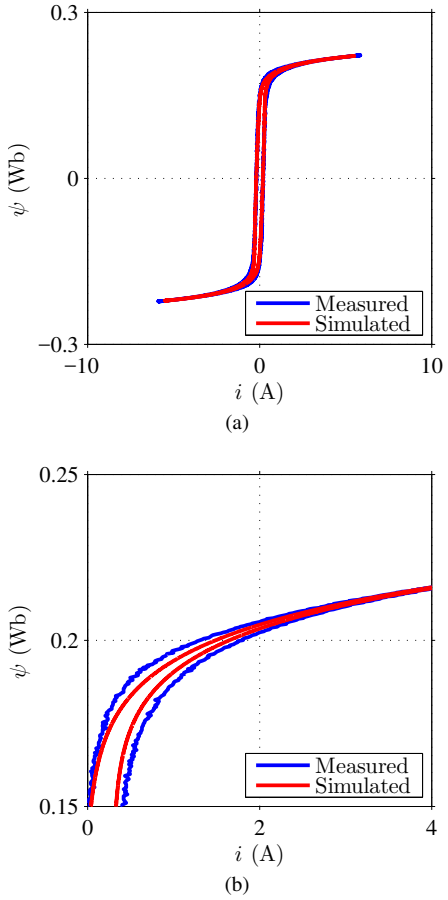

Fig. 7. Measured and simulated hysteresis loops at the excitation-voltage frequency of 100 Hz. The constant core-loss resistance $R_{\mathrm{Ft}} = 744.6$ Ω is used in the simulation model. The simulated loop is too narrow at higher flux values.

C. Comparison Between Measurements and Simulations

Simulations were performed in the Matlab/Simulink environment in order to compare the predicted waveforms to the measured ones. In Fig. 7, the hysteresis loop at the frequency of 100 Hz is shown when a constant resistor is used to model the core losses. The value of the resistance was 744.6 Ω as identified above for the proposed model. The constant-resistor model fits well at low flux values, however, at higher flux values the simulated loop is clearly too narrow. The estimated losses are thus lower than the actual losses. The corresponding results of the proposed model are shown in Fig. 8. As can be seen, the hysteresis loop obtained from the simulation data is in this case very similar to the measured hysteresis loop.

In Fig. 9, an example of minor hysteresis loops is shown. A 150-Hz voltage signal was superimposed on the 50-Hz input voltage. It can be seen that the minor loop produced by the proposed model agrees with the actual minor loop obtained from the measurement data. The same data as well as the voltage over the inductor are shown in time domain in Fig. 10.

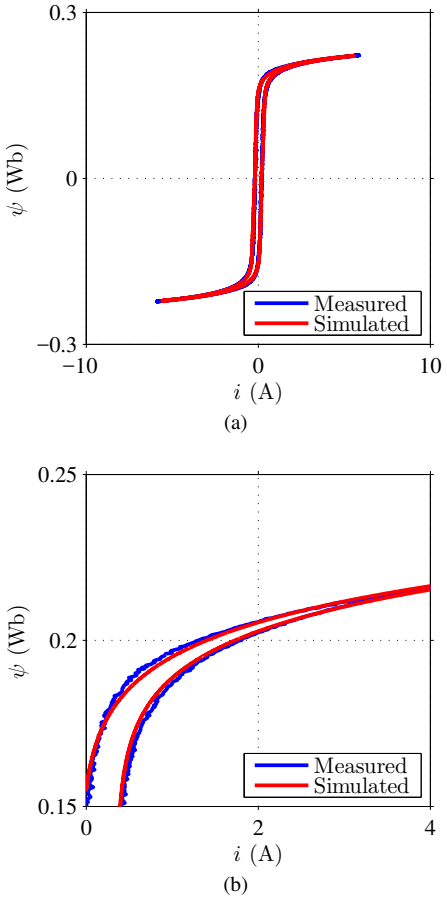

Fig. 8. Measured and simulated hysteresis loops at the excitation-voltage frequency of 100 Hz. The nonlinear core-loss resistor with the parameters $R_{\mathrm{Ft}} = 744.6\ \Omega$ and $\alpha = 315.2$ rad/s is used. Simulated loop agrees well with the measured data.

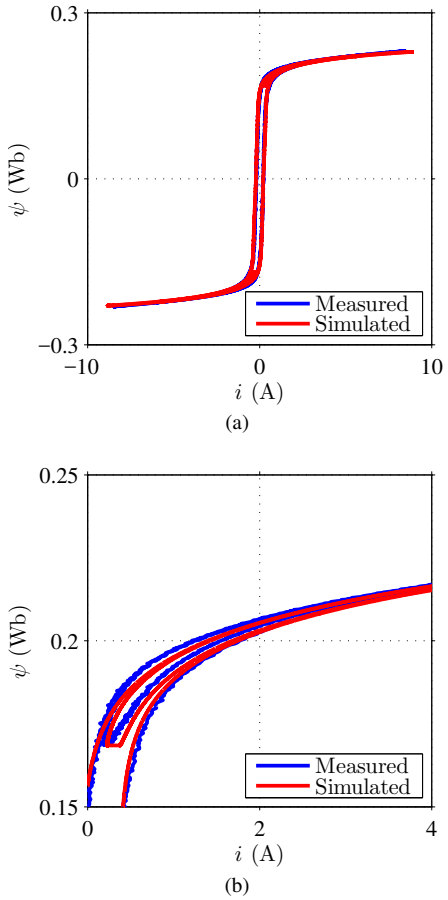

Fig. 9. Measured and simulated hysteresis loops at the excitation-voltage frequencies of 50 Hz and 150 Hz. The nonlinear core-loss resistor with the parameters $R_{\mathrm{Ft}} = 744.6\ \Omega$ and $\alpha = 315.2$ rad/s is used. Also the minor loops agree with the measured data.

V. Conclusions

In this paper, a dynamic model of a nonlinear hysteretic inductance was proposed. The model can be seen as a parallel combination of a nonlinear lossless inductance and a nonlinear resistance. The resistance model was derived based on the desired steady-state core-loss profile. The model was experimentally verified by hysteresis loop measurements of an electrical steel sample. It was shown, that the predicted hysteresis loop agrees very well with the measured data. The model is simpler than previously proposed models and easy to tune. The proposed model can be used in many applications, for instance in the modelling of core losses in AC machines.

Acknowledgement

The authors gratefully acknowledge the Academy of Finland and ABB Oy for the financial support.

References

[1] L. O. Chua and K. A. Stromsmoe, "Lumped-circuit models for nonlinear inductors exhibiting hysteresis loops," *IEEE Trans. Circuit Theory*, vol. CT-17, no. 4, pp. 564–574, Nov. 1970.

[2] ——, "Mathematical model for dynamic hysteresis loops," *Int. J. Eng. Sci.*, vol. 9, no. 5, pp. 435–450, May 1971.

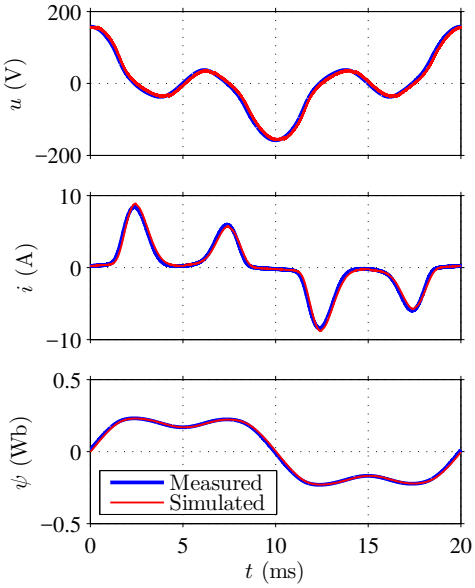

Fig. 10. Measured and simulated waveforms in time domain. Data correspond to that shown in Fig. 9.

[3] C. E. Lin, J.-G. Wei, C.-L. Huang, and C.-J. Huang, "A new model for transformer saturations characteristics by including hysteresis loops," *IEEE Trans. Magn.*, vol. 25, no. 3, pp. 2706–2712, May 1989.

[4] F. de León and A. Semlyen, "A simple representation of dynamic hysteresis losses in power transformers," *IEEE Trans. Power Delivery*, vol. 10, no. 1, pp. 315–321, Jan. 1995.

[5] M. S. Elkhatib and J. A. Barby, "Dynamic modelling of nonlinear energy storage elements and their applications to power electronics," in *Symp. IEEE MWSCAS'94*, Lafayette, Louisiana, Aug. 1994, pp. 1249–1252.

[6] N. Menemenlis, "Noniterative dynamic hysteresis modelling for real-time implementation," *IEEE Trans. Power Systems*, vol. 13, no. 4, pp. 1556–1563, Nov. 1998.

[7] M. Ranta, M. Hinkkanen, E. Dlala, A.-K. Repo, and J. Luomi, "Inclusion of hysteresis and eddy current losses in dynamic induction machine models," Miami, Florida, May 2009, pp. 1387–1392.

[8] H. C. J. de Jong, "Saturation in electrical machines," in *Proc. ICEM'80*, vol. 3, Athens, Greece, Sept. 1980, pp. 1545–1552.

[9] L. O. Chua, "Device modeling via basic nonlinear circuit elements," *IEEE Trans. Circuits Syst.*, vol. CAS-27, no. 11, pp. 1014–1044, Nov. 1980.

[10] M. Di Ventra, Y. V. Pershin, and L. O. Chua, "Circuit elements with memory: memristors, memcapacitors, and meminductors," *Proc. IEEE*, vol. 97, no. 10, pp. 1717–1724, Oct. 2009.